The Journal of Neuroscience, June 1, 1996, 16(11):3559–3570

IRK(1–3) and GIRK(1–4) Inwardly Rectifying K^+ Channel mRNAs Are Differentially Expressed in the Adult Rat Brain

Christine Karschin,[1] Elke Dißmann,[2] Walter Stühmer,[1] and Andreas Karschin[2]

[1]Molecular Biology of Neuronal Signals, Max-Planck-Institute for Experimental Medicine, and [2]Molecular Neurobiology of Signal Transduction, Max-Planck-Institute for Biophysical Chemistry, D-37075 Göttingen, Germany

Molecular cloning together with functional characterization has shown that the newly identified family of inwardly rectifying K^+ channels consists of several closely related members encoded by separate genes. In this report we demonstrate the differential mRNA expression and detailed cellular localization in the adult rat brain of seven members of the IRK and GIRK subfamilies. Using both radiolabeled cRNA riboprobes and specific oligonucleotide probes directed to nonconserved regions of both known and newly isolated rat brain cDNAs, *in situ* hybridization revealed wide distribution with partly overlapping expression of the mRNAs of IRK1–3 and GIRK1–4. Except for the low levels of GIRK4 transcripts observed, the overall distribution patterns of the other GIRK subunits were rather similar, with high levels of expression in the olfactory bulb, hippocampus, cortex, thalamus, and cerebellum. Marked differences in expression levels existed only in some thalamic, brainstem, and midbrain nuclei, e.g., the substantia nigra, superior colliculus, or inferior olive. In contrast, IRK subunits were expressed more differentially: all mRNAs were abundant in dentate gyrus, olfactory bulb, caudate putamen, and piriform cortex. IRK1 and IRK3 were restricted to these regions, but they were absent from most parts of the thalamus, cerebellum, and brainstem, where IRK2 was expressed predominantly. Because channel subunits may assemble as heteromultimers, additional functional characterization based on overlapping expression patterns may help to decipher the native K^+ channels in neurons and glial cells.

Key words: K_{IR} channel; inwardly rectifying; IRK; GIRK; K_{ATP} channel; in situ *hybridization heteromers; G-protein gating*

Inwardly rectifying K^+ (Kir) channels are involved in diverse cellular functions such as maintenance of the resting conductance, K^+ homeostasis, pacemaker activity, synaptic inhibition, and neuronal firing rates. Originally described in frog skeletal muscle, "anomalous" (Katz, 1949) or "inward" rectifiers favor the entry of K^+ during hyperpolarization and thus control the cell potential without causing massive loss of K^+ (Hille, 1992a; Jan and Jan, 1994). The recent molecular cloning of the first two channel subtypes from a macrophage cell line (Kubo et al., 1993a) and kidney (Ho et al., 1993) demonstrated a most primitive protein structure: hydropathy profiles of the primary amino acid sequences predicted only two transmembrane α-helices per subunit surrounding a putative pore-lining region. Since then, diverse cloning approaches have identified multiple new Kir family members from different tissues and species. On the basis of structure as well as physiological characteristics, these subtypes have been grouped tentatively into three major subfamilies (for a recent terminology, see Doupnik et al., 1995). First, ROMK-type (Kir1.0) channels are "mildly" rectifying, lack time-dependent gating, and are regulated by cytoplasmic ATP. Five splice variants are expressed predominantly in kidney but also are expressed in brain (Shuck et al., 1994; Yano et al., 1994; Zhou et al., 1994; Boim et al., 1995). Second, IRK-type (Kir2.0) channels are constitutively active with apparent time-dependent gating and "strong" inward rectification (Ishihara and Hiraoka, 1994; Stanfield et al., 1994). Structural similarities and unitary conductances further define IRK1 (Kir2.1: Morishige et al., 1993; Ishii et al., 1994; Wischmeyer et al., 1995b), IRK2 (Kir2.2: Koyama et al., 1994; Takahashi et al., 1994), and IRK3 subtypes (Kir2.3: Makhina et al., 1994; Morishige et al., 1994; Périer et al., 1994; Tang and Yang, 1994), which are likely to be expressed in the mammalian brain. Finally, the GIRK-type (Kir3.0) subfamily comprises four different channel subunits that are subject to G-protein activation. GIRK1 channels were first isolated from the rat atrium by expression cloning (Dascal et al., 1993; Kubo et al., 1993b) and found to be gated by $\beta\gamma$ subunits in a membrane-delimited manner (Reuveny et al., 1994; Wickman et al., 1994). More recently, two structurally related channels, mbGIRK2 and mbGIRK3, were identified from the mouse brain (Lesage et al., 1994). A fourth subtype (Kir3.4) was isolated from rat heart (Krapivinsky et al., 1995) and human hippocampus (Spauschus et al., 1996); this subtype probably does not underlie the previously described ATP-sensitive K_{ATP} channels, as had been assumed originally.

The observed multitude of genes together with the possible subunit assembly into heteromeric polypeptides may give rise to functionally diverse channel proteins, the majority of which are expressed in the mammalian brain. In this report we performed an extensive *in situ* hybridization study to describe the precise cellular distribution of IRK1–3 and GIRK1–4 channel subunits in the rat CNS.

Parts of this paper have been published in abstract form (Karschin et al., 1995).

MATERIALS AND METHODS

Molecular biology

To obtain sequence information on GIRK subunits of which no rat orthologs have been identified, a rat brain cDNA library (Stratagene, La Jolla, CA) was homology-screened under low stringency conditions as

Received Nov. 14, 1995; revised Feb. 5, 1996; accepted March 13, 1996.

This work was supported in part by the Deutsche Forschungsgemeinschaft "Synaptic Interaction in Neuronal Networks, SFB 406." We thank D. Reuter, G. Dowe, and R. Schubert for excellent technical assistance, Drs. H. A. Lester and N. Davidson for supplying the original GIRK1, and Dr. A. Parekh for critically reading the manuscript.

Correspondence should be addressed to Dr. Andreas Karschin, Molecular Neurobiology of Signal Transduction, Max-Planck-Institute for Biophysical Chemistry, 37077 Gottingen, Germany.

Copyright © 1996 Society for Neuroscience 0270-6474/96/163559-12$05.00/0

described by Spauschus et al. (1996). A total of $>3 \times 10^5$ clones were hybridized with either a [^{32}P]dCTP-labeled 2.1 kb fragment of rat heart GIRK1 (Dascal et al., 1993) or two 5′ cDNA fragments from the human hippocampus that coded for GIRK2 (1171 bp) and GIRK3 (387 bp; E. Dißmann, unpublished observations). Sequence analysis of positive clones identified full-length open reading frames (ORFs), which were likely to represent GIRK1, GIRK2, and GIRK3 rat orthologs. Rat brain GIRK1 was different from published sequences (Dascal et al., 1993; Kubo et al., 1993b) only in its 5′ and 3′ untranslated regions; rat brain GIRK2 was 98% similar to GIRK2 isolated from the mouse brain (Lesage et al., 1994) and identical to BIR1 (Bond et al., 1995) and K_{ATP}-2 (Stoffel et al., 1995), both isolated from pancreatic insulinoma cells; rat brain GIRK3 showed 99% amino acid identity to GIRK3 from the mouse brain.

In situ *hybridization*

In situ hybridization analysis was performed on rat and mouse brain sections using synthetic antisense and sense oligonucleotide probes. Experiments with cRNA probes specific for IRK1, GIRK1, and GIRK4 were carried out for comparison only and are not shown in the figures. Oligonucleotides of 44–50 bases in length were chosen from regions in the ORF or untranslated regions with least homology to other known Kir channels to minimize cross-hybridizations.

Specificity of probes. Except for IRK1, at least two subunit-specific antisense oligonucleotides corresponding to 3′ and 5′-end regions of the cDNA were generated. Identical hybridization patterns for each pair confirmed the specificity of the probes and minimized the risk that only possible splice variants were detected. Additional criteria for specific labeling were congruent data (1) in separate experiments and on more than three different brain sections, (2) between x-ray film images and emulsion dipped slides, and (3) matching mRNA expression patterns obtained with cRNA and oligonucleotide probes.

Effectiveness of oligonucleotide probes. All oligonucleotides were designed with the help of Lasergene software (DNAStar, Madison, WI) to guarantee oligonucleotides suited for hybridizations in terms of hairpin- and self-dimer formation. Only oligonucleotide probes that resulted in strong hybridization signals in any of the brain cells were considered to be effective and used for data analysis. Criteria for strong versus weak labeling of brain structures were the number of silver grains accumulated above cell somata relative to the strongest hybridization signal for a given oligonucleotide. Oligonucleotides designed for GIRK4, which detected only low mRNA expression levels in most brain regions, were found to reveal strong hybridization signals, e.g., in some selected vestibular nuclei neurons as well as in the rat heart.

Controls and background. The following controls were performed. Adjacent sections were (1) hybridized with sense riboprobes or sense oligonucleotides, (2) digested with RNase before hybridization, and (3) hybridized with a mixed oligonucleotide probe containing a 10-fold excess of cold probe. The silver grain densities observed in control sections were considered as background. Because only a few silver grains were present compared to specific signals over cell somata, no background subtractions were necessary.

The sequence and location (base position on coding strand indicated) of the oligonucleotides explicitly used for data analysis were as follows: IRK1: *antisense* ^{1263}5′TAAAGGCCTGGGCTCTAGAGGCACGCTCGCCTGGTTGTGGAGATCTATGC3′, *sense* ^{1214}5′GCATAGATCTCCACAACCAGGCGAGCGTGCCTCTAGAGCCCAGGCCTTTA3′ (cf. Wischmeyer et al., 1995b); IRK2: *antisense* ^{1467}5′GGTCATTCTGGCAATCCACCCTCCTGCCAACTTTCCCAAGCTATTGCAAG3′, *sense* ^{1417}5′CTTGCAATAGCTTGGGAAAGTTGGCAGGAGGGTGGATTGCCAGAATGACC3′ (cf. Koyama et al., 1994); IRK3: *antisense#1* ^{1251}5′CTCAAGCATCCGGATAATGCCTGCCTCCTCTTTGGAACCTGCCTCC3′ (cf. Morishige et al., 1994; three mismatches with rat IRK3), antisense#2 ^{48}5′TTTCCGCCTGGGCACGTGGGCCTGCCCGTTTCGGTTGTGTCCGT3′ (two mismatches with rat IRK3); GIRK1: *antisense* $^{-2}$5′AATACGGAGGGGAGATCCAGATTCAAACACGAAGCGGAGGCGCAGGAGCC3′ (cf. Dascal et al., 1993); *sense* ^{51}5′ GGCTCCTGCGCCTCCGCTTCGTGTTTGAATCTGGATCTCCCCTCCGTATT3′; GIRK2: *antisense* ^{1245}5′TCACCCATTCCTCTCCGTCAGTTCTTCCGGGTTCTTCTCTTCCTCTTCTG3′ (cf. Lesage et al., 1994; two mismatches with rat GIRK2); GIRK3: *antisense* ^{1131}5′TCAGCTCCATCTCCCGCACCTGCCCCCCTCCCCAGCCCCTTCTTCCTCCA3′ (cf. Lesage et al., 1994; two mismatches with rat GIRK3); GIRK4: *antisense#1* ^{48}5′ TCCAATCTCCATGTCCTGGTTCATGGCATTCCTAGAATCGCCAG3′ (GenBank accession number X83584); *antisense#2* ^{1173}5′CTCAGCACAGCCCCCCAGTGGGGGGGCTGGGGAGGTACTGGAGGAGC3′. Oligonucleotides were 3′ end-labeled with [^{35}S] dATP (DuPont/NEN, 1200 Ci/mmol) by terminal deoxynucleotidyl transferase (Boehringer Mannheim, Mannheim, Germany) and used for hybridization at concentrations of 2–10 pg/μl (400,000 cpm/100 μl hybridization buffer per slide). Alternatively, antisense and sense cRNA probes were generated with T3 and T7 RNA polymerase, respectively, by *in vitro* transcription using [^{35}S]UTP (Dupont/NEN; specific activities of $5–8 \times 10^8$ dpm/μg) from (1) GIRK1, a ~870 bp GIRK1 fragment including a 291 bp stretch of the 3′ ORF, (2) a ~1200 bp IRK1 fragment, and (3) a ~580 bp fragment covering the C-terminal region of the rat GIRK4 ORF.

For tissue preparation, adult Wistar rats and adult NMRI mice were anesthetized and decapitated, and the brain was removed and frozen quickly on dry ice. Timed pregnant rats were anesthetized and killed at various times of embryonic development (E16, E18, E20), and the embryos were removed and frozen. Adult brains and whole heads of embryos were cut on a cryostat at 10–16 μm, thaw-mounted onto Superfrost Plus slides, fixed with 4% paraformaldehyde in PBS, pH 7.4, dehydrated, and stored under ethanol until hybridization. For hybridizations with labeled oligonucleotides, slides were air-dried and hybridized overnight at 43°C in 100 μl buffer containing 50% formamide, 10% dextran sulfate, 50 mM DTT, 0.3 M NaCl, 30 mM Tris-HCl, 4 mM EDTA, 1× Denhardt's solution, 0.5 mg/ml denatured salmon sperm DNA, and 0.5 mg/ml polyadenylic acid. When sections were hybridized with cRNA riboprobes, slides were treated with proteinase K (1 μg/ml), acetylated with 0.25% acetic anhydride in 0.1 M triethanolamine, and prehybridized for 2 hr at 37°C in hybridization buffer (25 mM PIPES, pH 6.8, 0.75 M NaCl, 25 mM EDTA, 1× Denhardt's solution, 50% deionized formamide, 0.2% SDS, 100 mM DTT, 250 μg/ml denatured salmon sperm DNA, and 250 μg/ml polyadenylic acid). Subsequently, sections were incubated in the same hybridization buffer containing dextran sulfate (5%) and 0.02–0.2 ng/μl of the radiolabeled probe overnight at 54°C. Adjacent tissue sections were hybridized with sense riboprobes as controls. After hybridization with riboprobes, sections were washed twice in 4× SSC plus 50 mM β-mercaptoethanol for 15 min, treated with RNase A (50 μg/ml) for 30 min at 37°C, and washed twice with 2× SSC for 1 hr, followed by two 15 min high-stringency washes at 55–65°C in 0.1× SSC. Sections hybridized to oligonucleotide probes were washed twice for 30 min in 1× SSC plus 50 mM β-mercaptoethanol, 1 hr in 1× SSC at 60°C, and 10 min in 0.1× SSC at room temperature. Specimens were then dehydrated, air-dried, and exposed to Kodak BIOMAX x-ray film for 8–21 d. For cellular resolution, selected slides were subsequently dipped in photographic emulsion Kodak NTB2, incubated for 4–12 weeks, and then developed in Kodak D-19 for 2.5 min. For analysis with bright- and dark-field optics, sections were Nissl-counterstained with cresyl violet to confirm cytoarchitecture. Rat brain structures were identified and confirmed according to Paxinos and Watson (1986).

RESULTS

Data on the mRNA expression of IRK(1–3) and GIRK(1–4) Kir channels were compiled from examination of x-ray film images and emulsion-coated sections of five adult rat brains cut in sagittal, horizontal, and coronal planes. Table 1 summarizes the results for mRNA expression levels observed in the rat brain. GIRK1–3 subunits generally were expressed more strongly than the IRK-type subunits and showed a wide and highly overlapping distribution pattern (Fig. 1).

In sharp contrast, GIRK4 mRNA expression levels were low or nondetectable in most CNS regions. Both oligonucleotide and cRNA probes generally revealed similar expression patterns with most prominent transcript levels in the vestibular nuclei, superior colliculus, and habenula; in brain areas with very low transcription levels, such as the olfactory bulb and neocortex, GIRK4 mRNA was detected only with cRNA probes (Spauschus et al., 1996). Where possible, GIRK4 mRNA expression levels have been included in Table 1, but are otherwise not discussed in further detail.

IRK1,3 mRNAs were restricted noticeably to the forebrain and selected midbrain nuclei; in contrast, IRK2 mRNA was distributed throughout the brain with highest levels in cerebellum,

Table 1. Distribution of IRK/GIRK mRNAs in the CNS of the adult rat

Brain region	IRK1	IRK2	IRK3	GIRK1	GIRK2	GIRK3	GIRK4
Olfactory system							
Main olfactory bulb							
Granular cells	++	+	++	+++	++	+++	(+)
Mitral cells	+	+	++	+++	++	+++	(+)
Periglomerular cells	0	++	0	++	+	+++	(+)
Anterior olfactory nucleus	+	+	+++	++++	+++	++++	(+)
Olfactory tubercle	+++	+	+++	+	+	+++	(+)
Piriform cortex	++	++	+++	++++	+++	+++	(+)
Neocortex							
Cortical layer II	++	++	++	++++	+++	++++	(+)
Cortical layer III–VI	+	++	++	++++	+++	++++	(+)
Subiculum	+	++	++	+++	++	+++	(+)
Entorhinal cortex	++	++	++	++++	++	++++	(+)
Hippocampus							
Dentate gyrus granule cells	+++	++	+++	++++	++++	++++	(+)
Hilus dentate gyrus	0	0	+	+	+++	+++	(0)
CA1 pyramidal cells	+	++	+	+++	++++	++++	(+)
CA2 pyramidal cells			++				
CA3 pyramidal cells	0	0	0	++	+++	+++	(++)
Tenia tecta	+	±	+++	++++	+++	+++	(±)
Indusium griseum	0	+	++	+++	+++	+	(++)
Septum							
Bed nucleus stria terminalis	0	0	0	++	++	++	(0)
Lateral septal nucleus	±	±	0	+++	++	+	(++)
Basal ganglia							
Caudate putamen	+++	++	+++	+	0	++	(0)
Globus pallidus	0	0	0	+	0	+	(0)
Nucleus accumbens	+++	++	+++	+	0	+	(0)
Nucleus VDB	0	+++	0	+	+	+++	(n.d.)
Habenula	+	++++	0	++	++	++	(+++)
Amygdala	+	+	±	+++	+++	+++	(0)
Hypothalamus	+	+	0	+	+	++	(+)
Preoptic area	0	±	0	+	+	++	(0)
Supraoptic nucleus	0	++	0	0	0	++	(0
Mammillary nuclei	0	++	0	++	+	+	(0)
Substantia nigra							
Pars compacta	0	+	0	0	++++	++	(n.d.)
Pars reticulata	±	+	0	0	0	++	(n.d.)
Ventral tegmental area	0	0	0	0	+++	+	(n.d.)
Thalamus							
Thalamic reticular nucleus	0	++++	+++	+++	++	+++	(+)
Geniculate nucleus	0	++++	0	+++	+++	++++	(+)
Anterior nuclei (AD/AV)	0	++++	0	+++	+	++++	(+)
Lateral nuclei (LD/LP)	0	++++	0	+++	+++	++++	(+)
Ventroposterior nuclei (VP)	0	++++	0	+++	++	++++	(+)
Midbrain							
Superior colliculus	+++	+++	0	++	+	+++	(++)
Inferior colliculus	++	++	0	+++	±	+++	(0)
Central gray	+	+	0	+	+	++	(±)
APTD	+++	+	0	++	0	++	(n.d.)
DpMe	+++	++	0	+	+	++	(n.d.)
Oculomotor nucleus	0	++	0	+++	++	++	(n.d.)
Red nucleus	0	+	0	+++	++	+++	(n.d.)
Interpeduncular nucleus	n.d.	+	n.d.	+	0	++	(n.d.)
Cerebellum							
Deep nuclei	0	+	0	+++	0	+++	(0)
Molecular layer	0	0	0	+	0	++	(±)
Granule cell layer	0	++++	0	+++	++	+++	(++)
Purkinje cells	0	0	0	0	0	+++	(+)
Brainstem							
Pontine nucleus	++	+	0	+++	++	+++	(n.d.)
Trapezoid body	0	++	0	+++	0	+	(n.d.)
Inferior olivary nuclei	0	++++	0	0	0	++	(+)
Locus coeruleus	0	+	0	++	++	+++	(n.d.)
Raphé nuclei	0	+	0	±	0	++	(n.d.)
Pontine reticular formation	+	++	0	++	++	++	(n.d.)
Motor trigeminal nucleus	0	++++	0	++	++	+++	(n.d.)
Me5 cells	0	++	0	++	++	++	(n.d.)
Facial nucleus	+	++++	0	++	++	+++	(n.d.)
Vestibular nuclei	0	+	0	++	+++	+++	(++)
Cochlear nuclei	0	++++	0	+++	+++	+++	(n.d.)
Solitary nucleus	0	0	0	0	n.d.	++	(n.d.)
Cuneate nucleus	0	0	0	++	n.d.	++	(n.d.)
Dorsal tegmental nucleus	0	+	0	+	++	+++	(n.c.)
Lateral parabrachial nucleus	0	0	0	+	++	++++	(n.d.)
Hypoglossal nucleus	0	+++	0	+++	n.d.	++	(n.d.)
Spinal trigeminal nuclei	0	0	0	+++	++	+++	(n.d.)
	IRK1	IRK2	IRK3	GIRK1	GIRK2	GIRK3	GIRK4

In situ hybridization signals obtained for ^{35}S-labeled oligonucleotide probes on adult rat brain sections (dipped sections and x-ray film) were rated according to the relative grain density: ++++, very abundant; +++, abundant; ++, moderate; +, low; ±, just above background; 0, no expression; n.d., not determined. Ratings for GIRK4 were determined mainly from hybridizations with cRNA probes and therefore appear in parentheses. VDB, Nucleus vertical limb of the diagonal band; APTD, anterior pretactal nucleus; Me5, mesencephalic trigeminal nucleus; DpMe, deep mesencephalic nucleus.

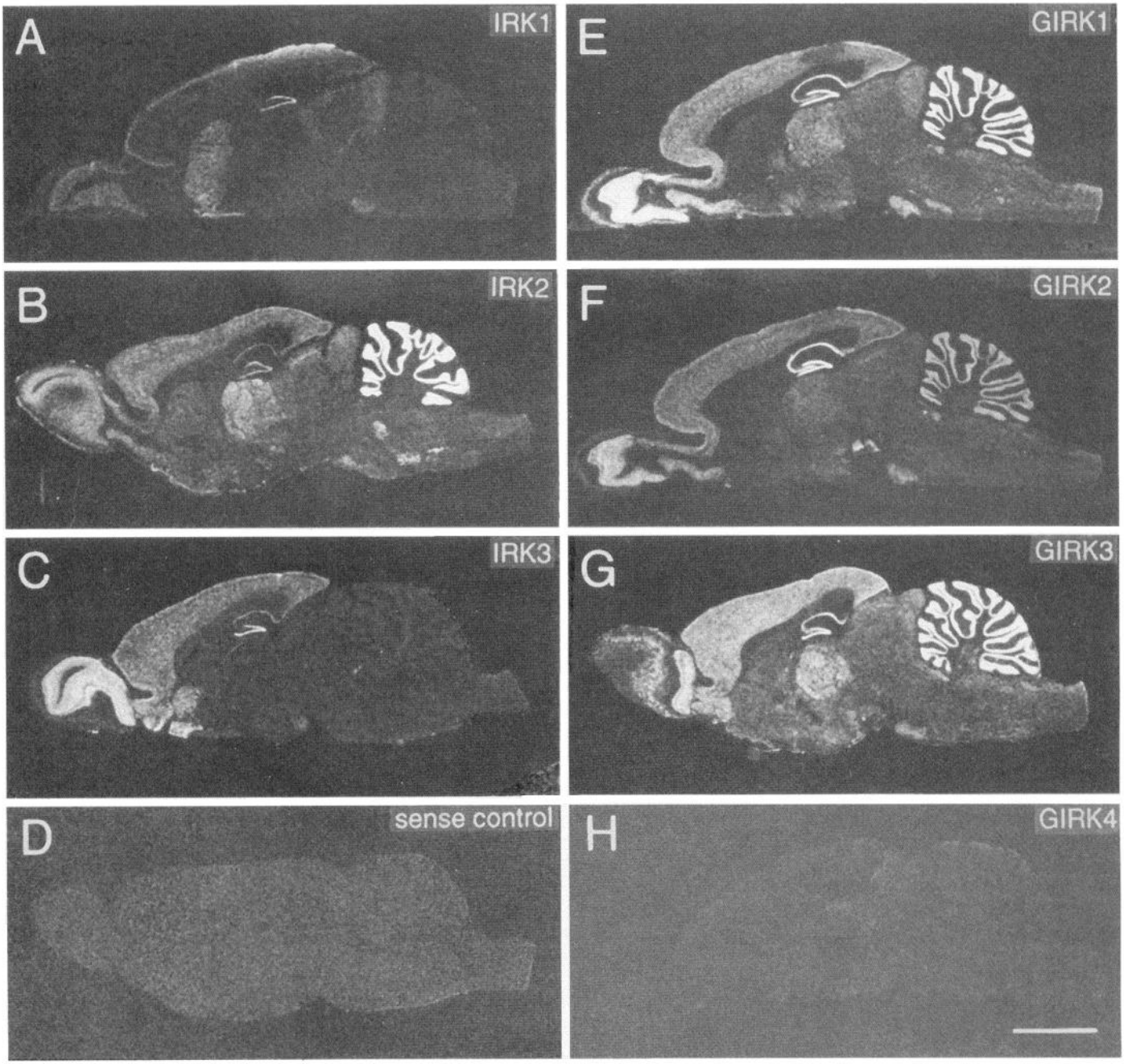

Figure 1. X-ray film images of sagittal rat brain sections show distribution of mRNAs as detected by *in situ* hybridization with oligonucleotide probes specific for IRK1 (*A*), IRK2 (*B*), IRK3 (*C*), GIRK1 (*E*), GIRK2 (*F*), GIRK3 (*G*), and GIRK4 (*H*). *D*, Control section hybridized with sense probe. Scale bar (shown in *H*): 5 mm. Exposure times are 8–21 d.

thalamus, and selected brainstem nuclei (Fig. 1). Appropriate controls performed with either sense oligonucleotide/RNA probes, a mixed probe with excess unlabeled oligonucleotides, or with tissue RNase-digested before hybridization revealed no specific labeling (Fig. 1*D*) for any of the probes and served as a measure of background labeling.

Both IRK1–3 and GIRK1–4 mRNAs were expressed in the developing brain as early as embryonic day 16 (data not shown). Overall, the embryonic expression patterns resembled the distribution in the adult brain; only IRK1-subunit mRNA levels were noticeably higher in the neocortical neuroepithelium compared with the adult cerebral cortex.

Olfactory system

All six subunit genes were expressed in the main olfactory bulb granular cell layer and mitral cell layer, but only IRK2 and GIRK3 mRNAs were abundant in glomerular cells. The anterior olfactory nucleus contained high levels of all GIRK subunits as well as IRK3 transcripts and weakly expressed IRK1,2 mRNAs. Although all subunit genes were expressed in the

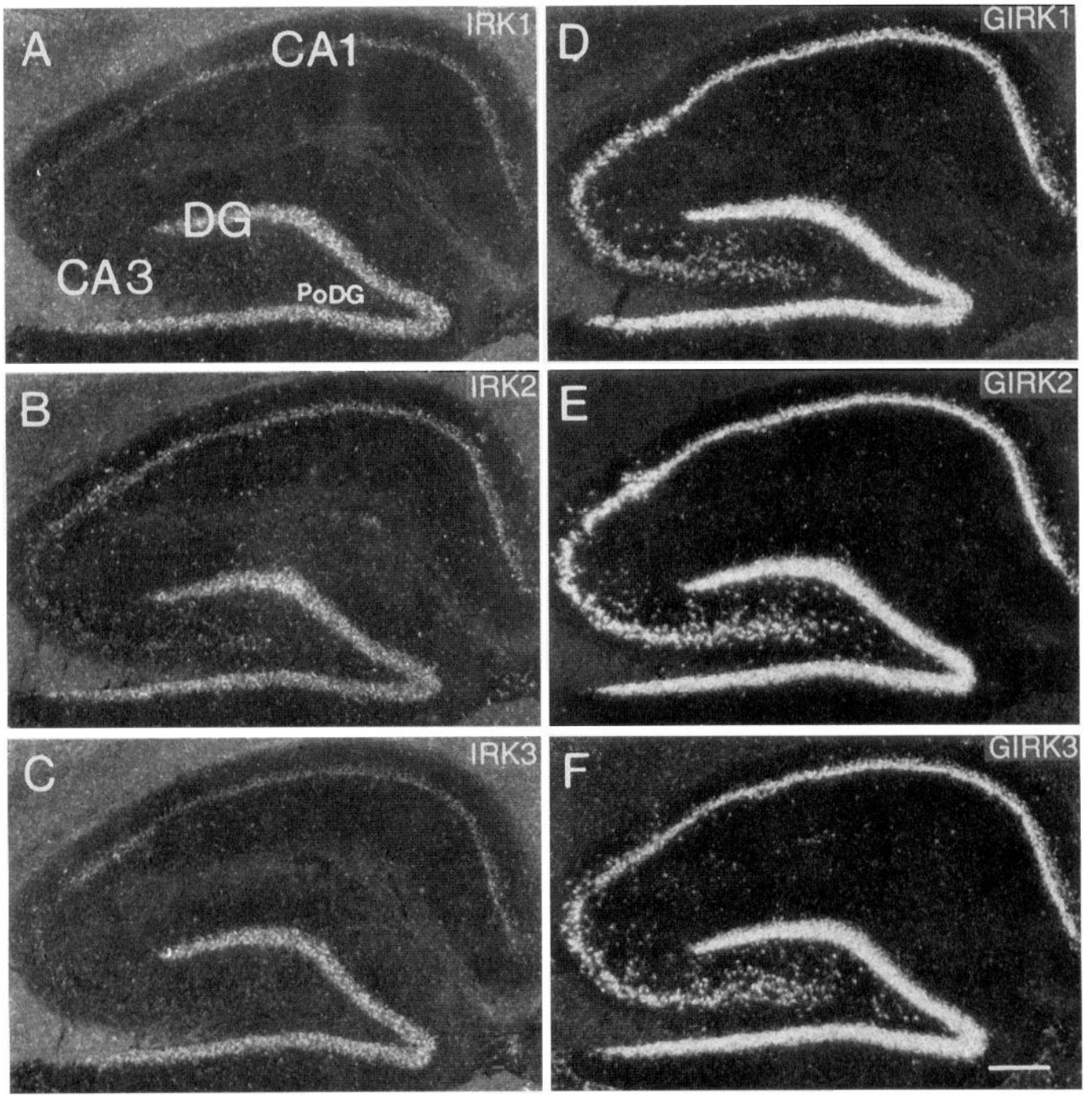

Figure 2. Dark-field photomicrographs of adjacent sagittal sections through the rat hippocampal region hybridized with oligonucleotides specific for IRK1 (*A*), IRK2 (*B*), IRK3 (*C*), GIRK1 (*D*), GIRK2 (*E*), and GIRK3 (*F*). *CA1, CA3*, Pyramidal cell layer of the CA1 and CA3 fields of the Ammon's horn; *DG*, granule cell layer of the dentate gyrus; *PoDG*, polymorphic layer of the dentate gyrus. Scale bar (shown in *F*): 300 μm.

piriform (primary olfactory) cortex, the olfactory tubercle was labeled prominently by IRK1,3 mRNAs and to a lesser extent by the other subunits.

Hippocampus

For the IRK family, transcripts were abundant only in dentate gyrus granule cells. Pyramidal cells of the CA1 region expressed low levels of all IRK subunits, whereas specific labeling basically was absent from CA3 neurons (Fig. 2*A–C*). IRK3 transcripts were found to be slightly elevated in the short CA2 stretch between the CA1 and CA3 neurons. This result was confirmed and even more conspicuous in mouse brain sections hybridized to the same oligonucleotide probe. All GIRK subunit genes, on the other hand, were expressed strongly by dentate gyrus granule cells as well as CA1–CA3 pyramidal neurons (Fig. 2*D–F*). A difference existed in the proximal hilus of the dentate gyrus, where large neurons contained significantly higher levels of GIRK2 and GIRK3 than GIRK1 mRNAs. Thus, in the hippocampus proper, different cell types seem to harbor strikingly different combinations of subunit

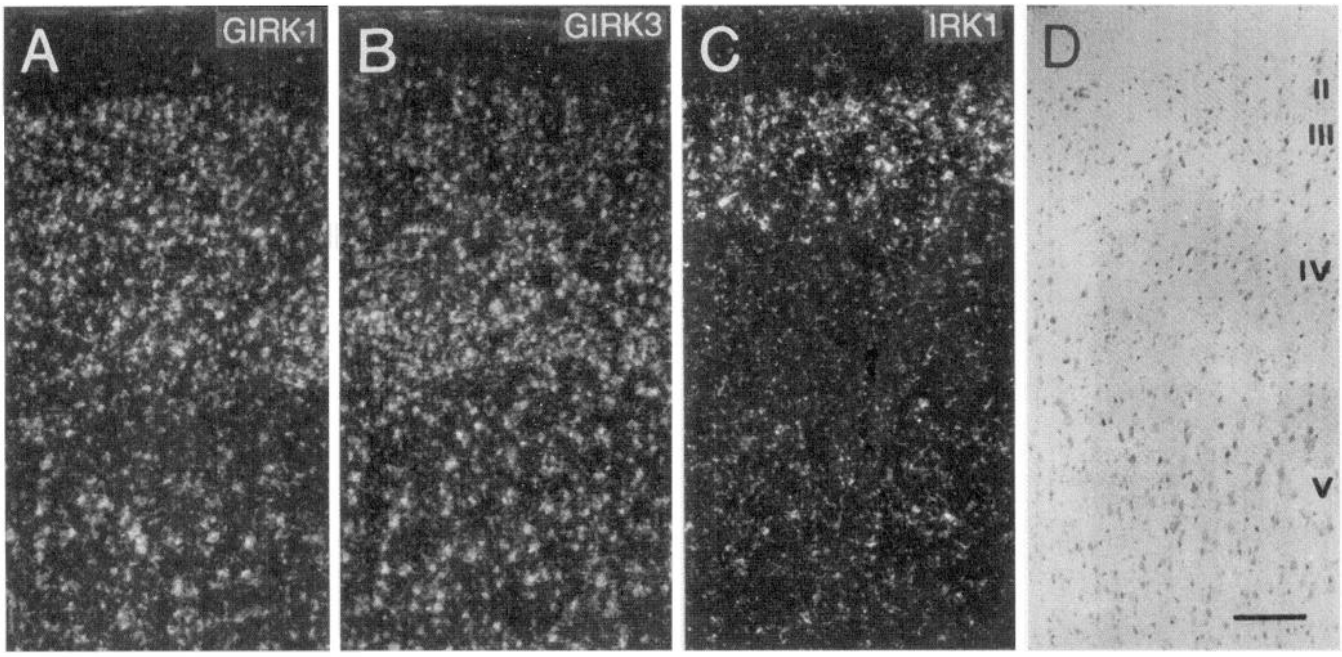

Figure 3. Dark-field photomicrographs of adjacent coronal sections through the parietal cortex hybridized with oligonucleotides specific for GIRK1 (*A*), GIRK3 (*B*), and IRK1 (*C*). *D*, Adjacent Nissl-stained section showing distribution of cells in cortical layers I–V. Scale bar (shown in *D*): 150 μm.

transcripts: some cells, such as dentate granule cells, express all six subunits, whereas others, e.g., some hilar neurons, express predominantly GIRK2 and/or GIRK3 subunits.

Neocortex

GIRK1–3 subunit genes were strongly expressed in all cortical areas with a labeling pattern reflecting the laminar structure of cell distribution as seen in Nissl-stained sections (Fig. 3*A,B*). Analysis of emulsion-dipped slides at high power showed that virtually all large cells, presumably pyramidal neurons, had accumulated silver grains above their somata. Thus we conclude that these subunits are coexpressed by most cortical pyramidal neurons. Although IRK2,3 mRNAs were present in all cortical layers at moderate levels, a more differential signal was observed for IRK1 mRNA, with particularly elevated levels in layer II neurons, but extremely low expression was observed in all other layers (Fig. 3*C*). All small cell bodies throughout the nuclear layers and white matter of the cortex, which probably represent oligo-, astro-, or microglia cells, failed to show hybridization signals for any of the Kir channels under study.

Basal ganglia and amygdala

The caudate putamen and nucleus accumbens were among the most prominently labeled brain structures when probed with IRK1,3 mRNAs. In both regions, virtually all small and medium-sized cells were labeled strongly (Fig. 4*A,B*). In contrast, IRK2 mRNA revealed a quite different expression pattern. Although most cells were found to be negative or weakly labeled, all of the large cells present exhibited prominent labeling (Fig. 4*C,D*). These cells are likely to represent the population of large aspiny cholinergic neurons that make up <2% of all cells in the caudate and seem immunoreactive to choline acetyltransferase antibodies (Paxinos, 1995). Interestingly, these large cells did not contain IRK1 mRNA (Fig. 4*B*). GIRK family members were absent in the basal ganglia (GIRK2), or only weak and diffuse expression was observed with GIRK1,3 mRNAs. Similarly, no expression of IRK mRNAs and low expression of GIRK1 and GIRK3 mRNAs were found in the globus pallidus. All three GIRK subunit mRNAs were expressed abundantly in amygdala nuclei. Although IRK2,3 mRNAs were absent, significant levels of IRK1 were found only in the central amygdaloid nucleus.

Thalamus

In the thalamus, a given subunit mRNA was expressed either by all nuclei (anterior, lateral, ventroposterior, and mediodorsal groups plus geniculate nuclei) or not at all. The only exception from this general observation was IRK3 mRNA, which was expressed solely in the reticular thalamic nucleus. IRK1 mRNA was not detected in any thalamic nucleus (Figs. 1*A*, 5*A*). GIRK1,3 and IRK2 subunit mRNAs were abundant in all thalamic nuclei, and GIRK2 mRNA was present at high levels in the lateral and geniculate nuclei and somewhat weaker in the other nuclei (Fig. 5*A–D*). As in cortex, all large neurons, but not the small, presumably glia cells, were intensely labeled, indicating coexpression of four subunits.

Substantia nigra (SN) and ventral tegmental area (VTA)

Only one subunit, GIRK2, was present at extremely high levels in the SN pars compacta and the adjacent VTA, but not in the pars reticulata (Fig. 6*A*). This cell population is likely to represent the group of dopaminergic neurons that make up 90% of all cells located in this area (Paxinos, 1995). The strong GIRK2 expression is particularly intriguing, because in the *weaver* mutant mouse, which features depletion of dopaminergic neurons in the pars compacta, a GIRK2 pore region mutation recently was shown to cause aberrant channel function (Patil et al., 1995). This GIRK channel subunit was found not to be as abundant in any other brain region, except for the hippocampus. GIRK3 mRNA was found throughout the SN and VTA, but with significantly lower levels when compared with GIRK2 (Fig. 6*B*). In contrast, GIRK1 and members of the IRK subfamily were absent (Fig. 6*C*) or weakly expressed by only a few cells.

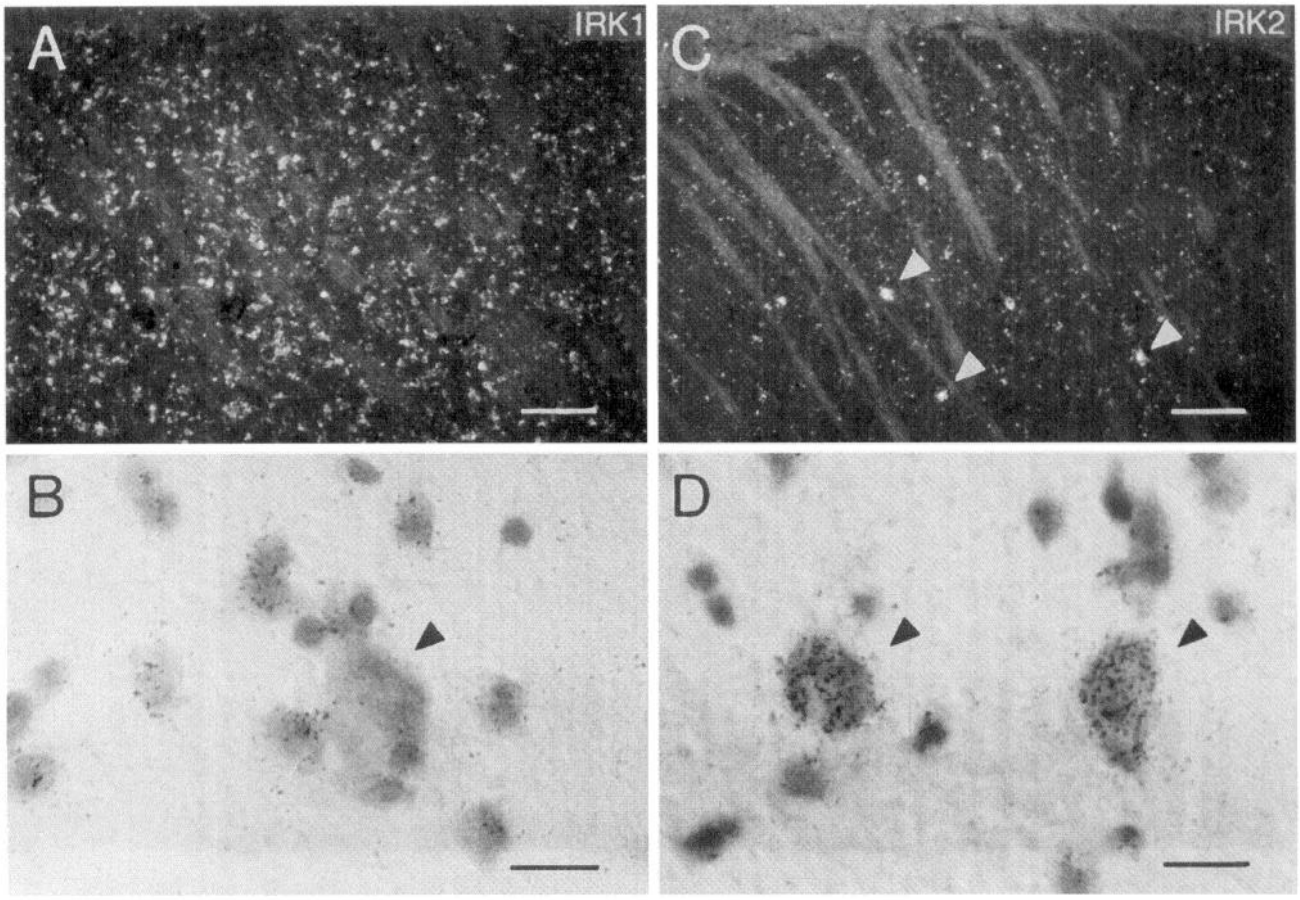

Figure 4. (*A, C*) Dark-field photomicrographs of sections through the caudate putamen hybridized with oligonucleotides specific for IRK1 (*A*) and IRK2 (*C*). Bright-field high-power photomicrographs in *B* and *D* demonstrate expression of IRK1 in most cells except the large neurons (*B*), whereas IRK2 mRNA is expressed predominantly by this population of large cells (*D*). Scale bars: *A, C*, 150 μm; *B, D*, 15 μm.

Superior and inferior colliculus

The inferior colliculus, the midbrain auditory relay station, contained high levels of GIRK1,3 mRNAs, whereas GIRK2 was absent. IRK1,2 genes were expressed moderately, and IRK3 mRNA was not detected. The superior colliculus (optic tectum) is the major target for retinal ganglion cells with horizontally laminated organization. The optic nerve layer contained very high levels of IRK1,2 and GIRK2 mRNAs, which is already apparent on the x-ray film images in Figure 1. GIRK1,3 mRNAs were also present in this layer but were not as conspicuous, because they were expressed as well in other layers. Expression in the central gray and deep mesencephalic nucleus was generally weak; however, in the latter, few cells were expressing very high levels of IRK1 mRNA, a subunit otherwise expressed rather moderately.

Cerebellum

A differential expression pattern was observed in the cerebellum. IRK1,3 mRNAs were not expressed (Fig. 1*A,C*); IRK2 mRNA expression was the strongest of all subunits and was restricted to granule cells. All three GIRK subunit genes were abundant in the granule cell layer, but although GIRK2 mRNA was found only in this layer, GIRK1,3 mRNAs also were expressed by cells in the molecular layer. Purkinje cells expressed only GIRK3 mRNA. The large neurons in the deep cerebellar nuclei contained high levels of GIRK1 and GIRK3 mRNAs and low levels of IRK2 transcripts.

Brainstem

All GIRK transcripts generally were abundant throughout the brainstem. In contrast, IRK3 mRNAs were absent, and IRK1 mRNAs were expressed only in the pontine and facial nucleus (compare Fig. 1*A*). A special feature of IRK2 was the generally weak mRNA expression with extremely high levels in a few selected nuclei, e.g., motor trigeminal nucleus (Fig. 7), facial nucleus, cochlear nuclei, hypoglossus nucleus, and the inferior olive (Fig. 8).

DISCUSSION

The wide expression in the adult rat brain of most of the seven tested Kir channel mRNA transcripts may be an indication of their important roles in central signal processing. Because ROMK1 (Kir1.1) transcripts were found to be expressed most weakly in nervous tissue (Karschin et al., 1994; Kenna et al., 1994; Yano et al., 1994; Boim et al., 1995), we refrained from giving a detailed description of this and other ROMK splice variants. Members of the other subfamilies, however, are expressed widely in various brain areas. Overall, the distribution patterns of the GIRK subunits, except GIRK4, were quite similar, with marked differences only in some thalamic, midbrain, and brainstem nuclei. Together with physiological evidence, the extremely low abundance of GIRK4 mRNA transcripts in the rat brain may favor the view that GIRK4 does not represent the long-sought and widely distributed K_{ATP} channel (Krapivinsky et al., 1995; Spauschus et

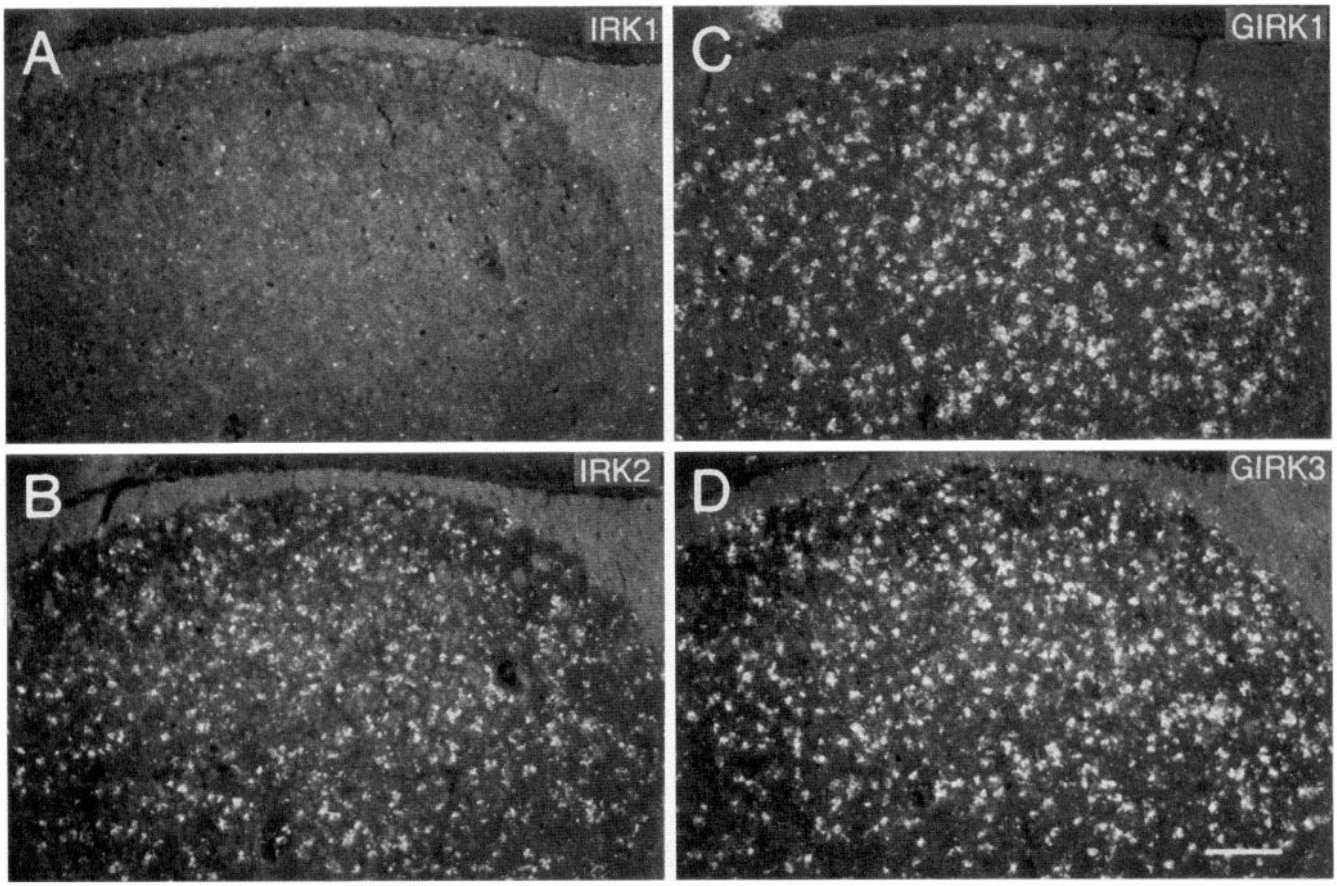

Figure 5. Dark-field photomicrographs of adjacent sections through the region of the dorsal lateral geniculate of the rat thalamus hybridized to (*A*) IRK1-, (*B*) IRK2-, (*C*) GIRK1-, and (*D*) GIRK3-specific oligonucleotides. Scale bar (shown in *D*): 150 μm.

al., 1996). In comparison, IRK1, IRK2, and IRK3 subunits were abundant and expressed quite differentially, with most distinct expression in the thalamus, cerebellum, and brainstem.

Selective hybridization and a more precise cellular localization was guaranteed in this report by the use of at least two specific oligonucleotide probes for each subunit directed to nonconserved regions in either the coding or the untranslated sequences of the genes. Our results with GIRK1 oligonucleotides coincide with the expression pattern revealed by full-length riboprobes in rat (Karschin et al., 1994) and mouse brain (Kobayashi et al., 1995). The distribution of GIRK2 mRNA transcripts in the mouse (Kobayashi et al., 1995) was similar to that in the rat, except for its absence in the thalamus; however, in contrast to our report, GIRK3 signals were found to be absent in the mouse brain olfactory bulb, hippocampus, and caudate putamen. Even more substantial differences from our report on mRNA expression levels were obtained for IRK1 riboprobes, particularly in the olfactory glomeruli, cerebellum, and hippocampus (Morishige et al., 1993); however, in control experiments using IRK1 riboprobes on rat brain and oligonucleotides on mouse brain sections (C. Karschin, unpublished observations), we could not confirm an apparent species discrepancy but found identical results in the mouse and rat brain. The present study also reveals a much more differential expression pattern of IRK3 mRNA transcripts than that described by Falk et al. (1995), who used fluorescein-labeled cRNA probes. These authors report a widely distributed moderate labeling throughout the rat brain, with highest expression levels in the tenia tecta, indusium griseum, piriform cortex, cerebellar Purkinje cells, and hippocampal cell layers. In contrast to their report and in strong agreement with a previous study on IRK3 (BIRK2) mRNA expression in the rat brain (Bredt et al., 1995), we found IRK3 subunit mRNAs limited to the forebrain and basically absent from CA3 pyramidal cells, cerebellum, brainstem, and almost all thalamic and midbrain nuclei. In the first description of IRK3 from the mouse brain (Morishige et al., 1994), Northern blot analysis detects IRK3 mRNA specifically in the forebrain but not in the cerebellum. Because both antisense oligonucleotides used in our study were derived from this sequence and showed two and three mismatches to the rat sequence, we also performed *in situ* hybridizations on mouse brain sections to detect possible differences (data not shown). As expected for closely related animal species, the distribution of IRK3 mRNA was identical in the rat and mouse brain. These results indicate that for a reliable comparison of data, it is important that great care be taken to confirm that (1) riboprobes do not cross-hybridize with RNAs of other family members and (2) alternative labeling techniques do not introduce nonspecific background staining, particularly in regions of high cell density.

As for other ion channels and membrane receptors that belong to multimember protein families, it remains a challenge to interpret mRNA distribution patterns and possibly deduce functional significance from the expression of Kir subunits in a given cell. (1) When anatomical and physiological data are compared, what appears as a homogenous macroscopic current in whole-cell patch-clamp or intracellular recordings in fact may be a composite of several different Kir conductances. Examples exist both in

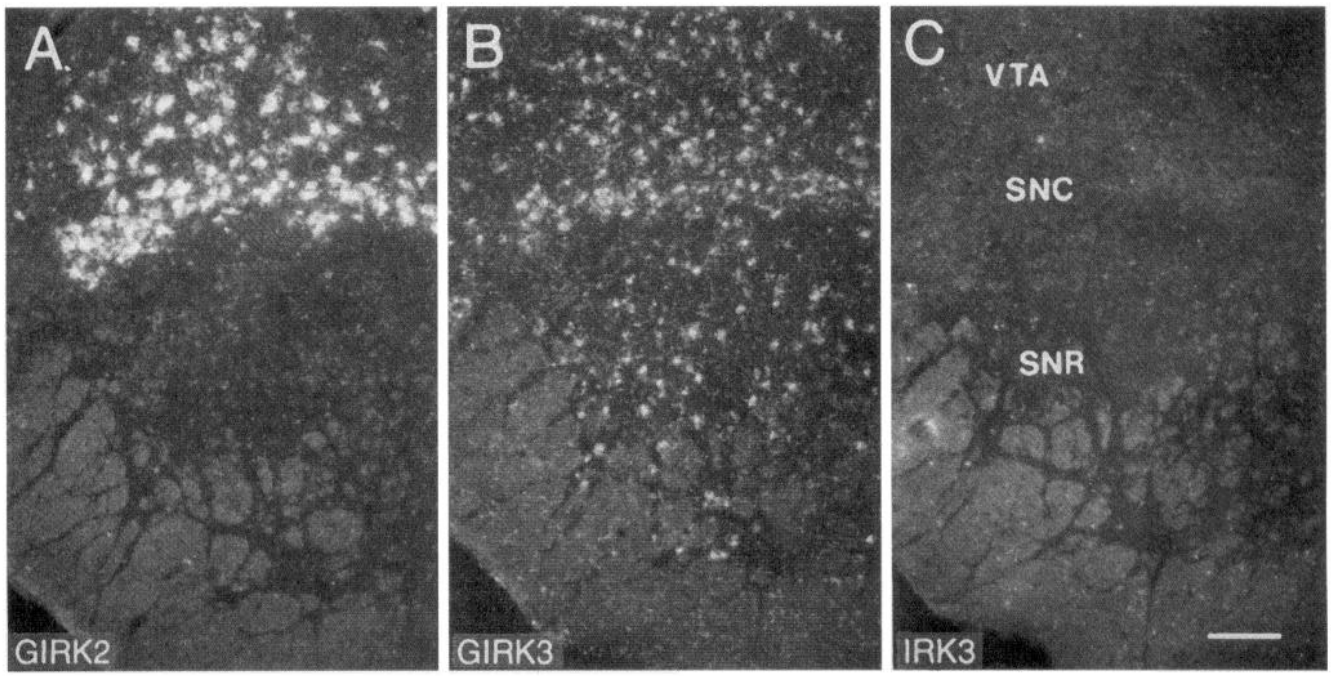

Figure 6. Dark-field photomicrographs of adjacent sagittal sections through the rat SN and VTA hybridized to oligonucleotides specific for GIRK2 (*A*), GIRK3 (*B*), and IRK3 (*C*). Note the intense labeling of putatively dopaminergic neurons with GIRK2 mRNA. *VTA*, Ventral tegmental area; *SNC*, substantia nigra pars compacta; *SNR*, substantia nigra pars reticulata. Scale bar (shown in *C*): 150 μm.

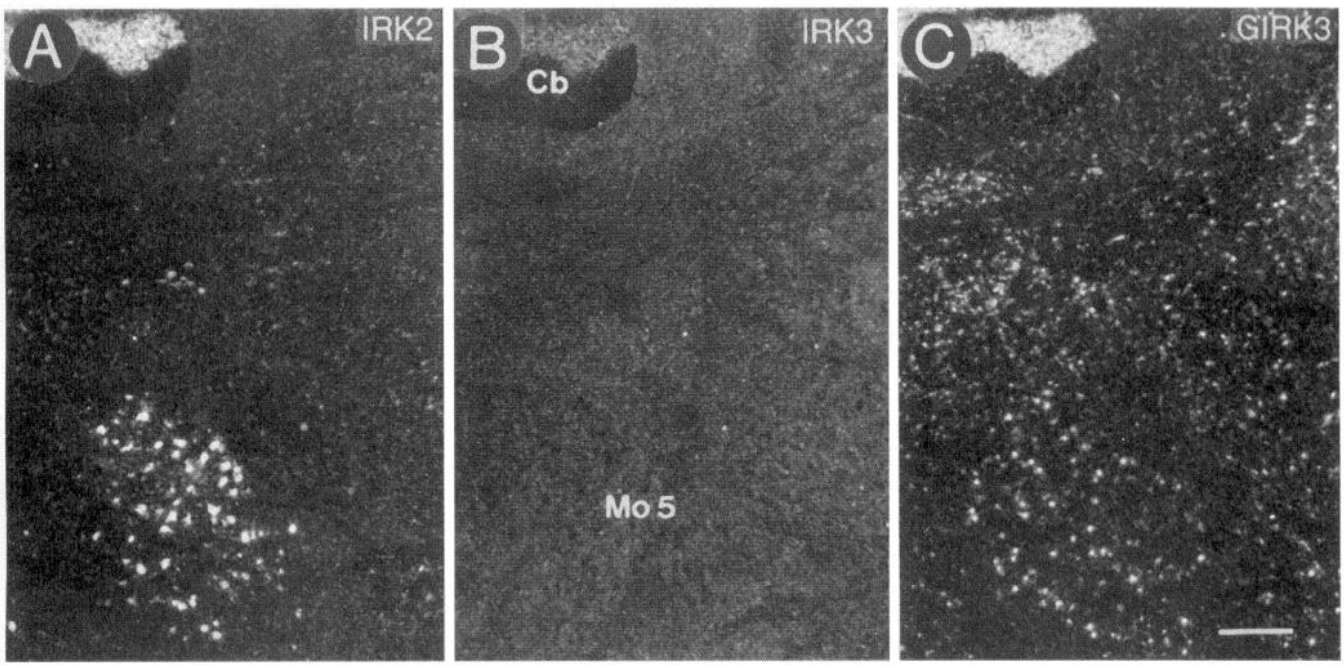

Figure 7. Dark-field photomicrographs of adjacent sections through the rat upper brainstem region hybridized to oligonucleotides specific for IRK2 (*A*), IRK3 (*B*), and GIRK3 (*C*). For orientation, part of a cerebellar lobe (*Cb*) is shown in the *upper left corner*. IRK2 mRNA expression is restricted to the motor trigeminal nucleus (*Mo5*), GIRK3 mRNA is abundantly expressed throughout the brainstem region, and IRK3 is completely absent from this area. Scale bar (shown in *C*): 300 μm.

central neurons (VanDongen et al., 1988; Penington et al., 1993) and in glial cells (Barres et al., 1988; Karschin and Wischmeyer, 1995). The features of recombinant Kir subtypes together with their differential localization thus may help to narrow down the molecular identity of native channels. (2) In addition to the existence of multiple genes and splice variants, functional diversity of Kir channels may arise if native channels assemble as heterotetrameric polypeptides. GIRK subunits form heteromeric channels in the mammalian heart (muscarinic K_{ACh} channels; Krapivinsky et al., 1995) and are likely to do so in the CNS *in vivo* (Duprat et al., 1995; Kofuji et al., 1995; Spauschus et al., 1996). Therefore, where overlapping mRNA expression is identified, e.g., in hippocampal CA3 neurons, data obtained from native cells could be compared with the functional coexpression of the respective

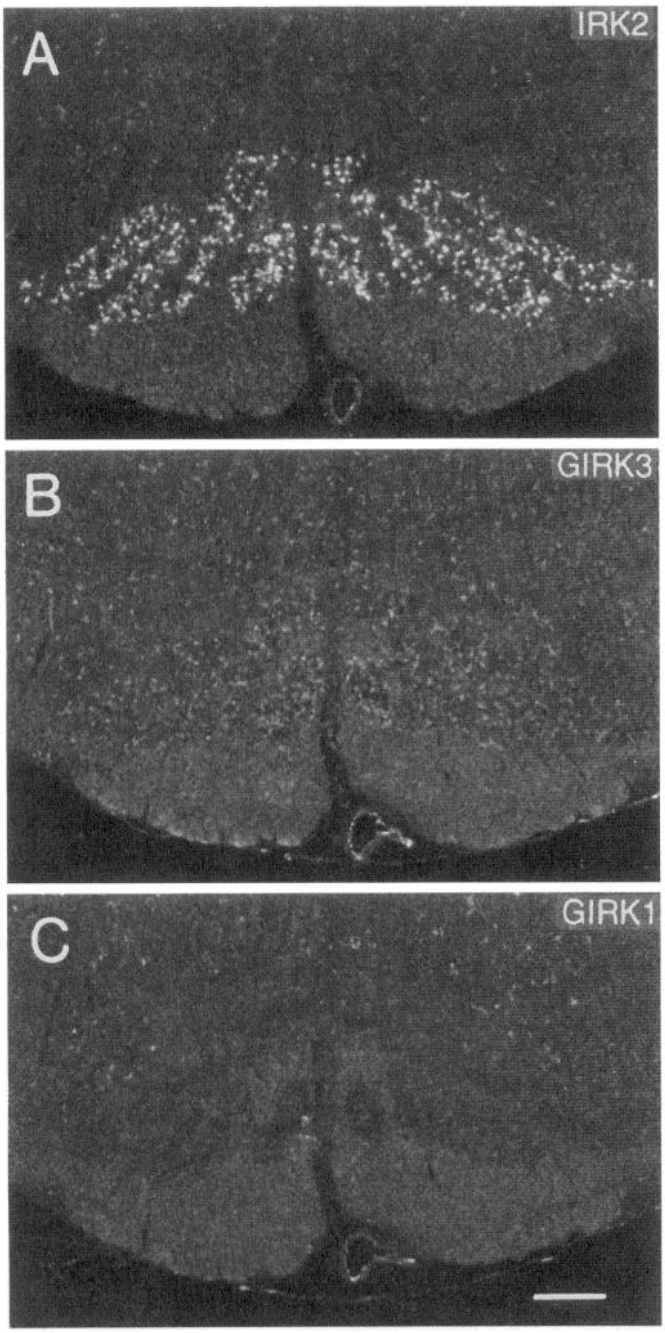

Figure 8. Dark-field photomicrographs of coronal sections through the lower brainstem. Note that neurons in the inferior olive are intensely labeled with IRK2 (*A*), moderately express GIRK3 mRNA (*B*), and do not express GIRK1 mRNA (*C*). Scale bar (shown in C): 300 μm.

cloned Kir channel subunits. Elucidation of the cellular RNA expression patterns that can be obtained from single-cell PCR (Lambolez et al., 1992) or aRNA amplification assays (Eberwine et al., 1992; Karschin, 1995) additionally may support this analytical approach.

Immunohistochemical studies on the localization of members of other K^+ channel families indicate that the use of subunit-specific antibodies may achieve a subcellular resolution beyond that revealed by mRNA *in situ* hybridizations. A complex differential subcellular distribution, for instance, has been shown for two voltage-gated K^+ channel subunits, Kv1.1 and Kv1.2 (Sheng et al., 1994; Wang et al., 1993, 1994). Interestingly, both subunits are restricted to different cellular regions in different cells; e.g., Kv1.2 seems to be concentrated exclusively in the dendrites of cortical and hippocampal pyramidal cells but is localized predominantly in the nerve terminals of cerebellar basket cells. Consequently, Kv1.2 may participate in distinct heteromultimeric K^+ channels and thus may play diverse functional roles in different subcellular domains, depending on the cell type; a similar scenario may be hypothesized for the various Kir channel subunits.

In addition to generating a constitutive basal K^+ conductance, Kir channels in the brain function as a major target for G-protein-mediated receptor function. Signal transduction from G-protein-coupled "7-helix receptors" to IRK and ROMK channels may be both excitatory and inhibitory and primarily occurs via classical cytoplasmic pathways that involve the action of one or several enzymes, including a final phosphorylation/dephosphorylation process (Fakler et al., 1994; McNicholas et al., 1994; Wischmeyer et al., 1995a). Alternatively, GIRK-type channels are opened through direct coupling of activated $G\beta\gamma$ subunits in a membrane-delimited process, apparently without involving cytoplasmic second messengers (Brown, 1993; Clapham, 1994; Reuveny et al., 1994; Wickman et al., 1994). In many cases, these two basic signal transduction schemes are difficult to distinguish experimentally. Therefore, except for the most thoroughly examined neurons, e.g., hippocampal pyramidal neurons, locus coeruleus, and nucleus basalis neurons (Nakajima et al., 1988; VanDongen et al., 1988; Velimirovic et al., 1995), it has not been possible to define uneqivocally the nature of the Kir channels involved.

In the brain, Kir channels are activated by the stimulation of muscarinic m2, α2 adrenergic, D2 dopamine, histamine, serotonin 1A, A1 adenosine, $GABA_B$, μ-, κ-, and δ-opioid, somatostatin, and possibly other receptors (North, 1989; Hille, 1992b). Single-channel analysis revealed some physiological inhomogeneities among the target channels involved. Somatostatin-activated 55 pS Kir channels were characterized in immortalized pituitary cells (Pennefather et al., 1987; Yatani et al., 1987;), and various other channels of 33 pS (Grigg et al., 1992), 45 pS (Miyake et al., 1989) and 80 pS conductance (Brown, 1990) are stimulated by somatostatin, opioids, and norepinephrine in locus coeruleus neurons (all three GIRK subtypes expressed). In hippocampal pyramidal neurons, in which our report has identified each of the four GIRK subunits tested (including all IRK subunits), a subpopulation of G_o-gated Kir channels possibly activated by serotonin, adenosine, or $GABA_B$ receptors showed a 38–42 pS conductance level, which agrees well with the native and recombinant GIRK1/4 channels of the heart atrium (VanDongen et al., 1988; Dascal et al., 1993; Krapivinsky et al., 1995). In this report, we find neurons of the dorsal raphé nucleus to be labeled positively for IRK2 and GIRK3 mRNA transcripts. When they were isolated acutely, these neurons exhibited a complex pattern of partial serotonin-activated conductances of 11, 21, 30, and 40 pS at the single-channel level (Penington et al., 1993).

A detailed cellular localization of Kir channel subunits may help to correlate subtype expression and single-channel characteristics. Nevertheless, additional characterization will be required to determine whether functional differences are based on the differential distribution of IRK and GIRK subfamily members, splice variants that may exist in the brain, heteromeric channel proteins, or cell-specific regulation by accessory proteins, as has been documented for the interaction between inhibitory sulfonylurea receptors and K_{ATP} channels (Aguilar-Bryan et al., 1995).

REFERENCES

Aguilar-Bryan L, Nichols CG, Wechsler SW, Clement IV JP, Boyd III AE, González G, Herrera-Sosa H, Nguy K, Bryan J, Nelson DA (1995) Cloning of the β cell high-affinity sulfonylurea receptor: a regulator of insulin secretion. Science 268:423–426.

Barres BA, Chun LL, Corey DP (1988) Ion channel expression by white matter glia: I. Type II astrocytes and oligodendrocytes. Glia 1:10–30.

Boim MA, Ho K, Shuck ME, Bienkowski MJ, Block JH, Slightom JL, Yang Y, Brenner BM, Hebert SC (1995) ROMK inwardly rectifying ATP-sensitive K^+ channel. II. Cloning and distribution of alternative forms. Am J Physiol 268:F1132–F1140.

Bond CT, Ämmälä C, Ashfield R, Blair TA, Gribble F, Khan RN, Lee K, Proks P, Rowe ICM, Sakura H, Ashford MJ, Adelman JP, Ashcroft FM (1995) Cloning and functional expression of the cDNA encoding an inwardly rectifying potassium channel expressed in pancreatic β-cells and the brain. FEBS Lett 367:61–66.

Bredt DS, Wang T, Cohen NA, Guggino WB, Snyder SH (1995) Cloning and expression of two brain-specific inwardly rectifying potassium channels. Proc Natl Acad Sci USA 92:6753–6757.

Brown AM (1993) Membrane-delimited cell signaling complexes: direct ion channel regulation by G proteins. J Membr Biol 131:93–104.

Brown DA (1990) G proteins and potassium currents in neurons. Annu Rev Physiol 52:215–242.

Clapham DE (1994) Direct G protein activation of ion channels? Annu Rev Neurosci 17:441–464.

Dascal N, Schreibmayer W, Lim NF, Wang W, Chavkin C, DiMagno L, Labarca C, Kieffer BL, Gaveriaux-Ruff C, Trollinger D, Lester HA, Davidson N (1993) Atrial G protein-activated K^+ channel: expression cloning and molecular properties. Proc Natl Acad Sci USA 90:10235–10239.

Doupnik CA, Davidson N, Lester HA (1995) The inward rectifier potassium channel family. Curr Opin Neurobiol 5:268–277.

Duprat F, Lesage F, Guillemare E, Fink M, Hugnot JP, Bigay J, Lazdunski M, Romey G, Barhanin J (1995) Heterologous multimeric assembly is essential for K^+ channel activity of neuronal and cardiac G-protein-activated inward rectifiers. Biochem Biophys Res Commun 212:657–663.

Eberwine J, Yeh H, Miyashiro K, Cao Y, Nair S, Finnell R, Zettel M, Coleman P (1992) Analysis of gene expression in single live neurons. Proc Natl Acad Sci USA 89:3010–3014.

Fakler B, Brändle U, Glowatzki E, Zenner HP, Ruppersberg JP (1994) Kir2.1 inward rectifier K^+ channels are regulated independently by protein kinases and ATP hydrolysis. Neuron 13:1413–1420.

Falk T, Meyerhof W, Corrette BJ, Schäfer J, Bauer CK, Schwarz JR, Richter D (1995) Cloning, functional expression and mRNA distribution of an inwardly rectifying potassium channel protein. FEBS Lett 36:127–131.

Grigg JJ, Kozasa T, Nakajima Y, Nakajima S (1992) Single channel properties of the inwardly rectifying K-current activated by somatostatin or Met-enkephalin in cultured rat brain neurones (Abstr). Biophys J 61:A14.

Hille B (1992a) Ionic channels of excitable membranes. Sunderland, MA: Sinauer.

Hille B (1992b) G protein-coupled mechanisms and nervous signaling. Neuron 9:187–195.

Ho K, Nichols CG, Lederer WJ, Lytton J, Vassilev PM, Kanazirska MV, Hebert SC (1993) Cloning and expression of an inwardly rectifying ATP-regulated potassium channel. Nature 362:31–38.

Ishihara K, Hiraoka M (1994) Gating mechanism of the cloned inward rectifier potassium channel from mouse heart. J Membr Biol 142:55–64.

Ishii K, Yamagashi T, Taira N (1994) Cloning and functional expression of a cardiac inward rectifier K^+ channel. FEBS Lett 338:107–111.

Jan LY, Jan YN (1994) Potassium channels and their evolving gates. Nature 371:119–122.

Karschin A (1995) Molecular single-cell analysis identifies somatostatin type 1 (sst1) receptors to block inwardly rectifying K^+ channels in rat brain oligodendrocytes. NeuroReport 7:121–124.

Karschin C, Schreibmayer W, Dascal N, Lester H, Davidson N, Karschin A (1994) Distribution and localization of a G protein-coupled inwardly rectifying K^+ channel in the rat. FEBS Lett 348:139–144.

Karschin A, Wischmeyer E (1995) Identification of G protein-regulated inwardly rectifying K^+ channels in rat brain oligodendrocytes. Neurosci Lett 183:135–138.

Karschin C, Dißmann E, Stühmer W, Karschin A (1995) Expression and cellular localization of six members of the GIRK and IRK family of inwardly rectifying K^+ channels. Soc Neurosci Abstr 21:1325.

Katz B (1949) Les constantes électriques de la membrane du muscle. Arch Sci Physiol 2:285–299.

Kenna S, Röper J, Ho K, Hebert S, Ashcroft SJH, Ashcroft FM (1994) Differential expression of the inwardly rectifying K-channel ROMK1 in rat brain. Mol Brain Res 24:353–356.

Kobayashi T, Ikeda K, Ichikawa T, Abe S, Togashi S, Kumanishi T (1995) Molecular cloning of a mouse G-protein-activated K^+ channel (mGIRK1) and distinct distributions of three GIRK (GIRK1, 2 and 3) mRNAs in mouse brain. Biochem Biophys Res Commun 208:1166–1173.

Kofuji P, Davidson N, Lester HA (1995) Evidence that neuronal G-protein-gated inwardly rectifying K^+ channels are activated by $G\beta\gamma$ subunits and function as heteromultimers. Proc Natl Acad Sci USA 92:6542–6546.

Koyama H, Morishige KI, Takahashi N, Zanelli JS, Fass DN, Kurachi Y (1994) Molecular cloning, functional expression and localization of a novel inward rectifier potassium channel in the rat brain. FEBS Lett 341:303–307.

Krapivinsky G, Gordon EA, Wickman K, Velimirovic B, Krapivinsky L, Clapham DE (1995) The G-protein-gated atrial K^+ channel I_{KACh} is a heteromultimer of two inwardly rectifying K^+-channel proteins. Nature 374:135–141.

Kubo Y, Baldwin TJ, Jan YN, Jan LY (1993a) Primary structure and functional expression of a mouse inward rectifier potassium channel. Nature 362:127–133.

Kubo Y, Reuveny E, Slesinger PA, Jan YN, Jan LY (1993b) Primary structure and functional expression of a rat G-protein-coupled muscarinic potassium channel. Nature 364:802–806.

Lambolez B, Audinat E, Bochet P, Crépel F, Rossier J (1992) AMPA receptor subunits expressed by single Purkinje cells. Neuron 9:247–258.

Lesage F, Duprat F, Fink M, Guillemare E, Coppola T, Lazdunski M, Hugnot JP (1994) Cloning provides evidence for a family of inward rectifier and G-protein coupled K^+ channels in the brain. FEBS Lett 353:37–42.

Makhina EN, Kelly AJ, Lopatin AN, Mercer RW, Nichols CG (1994) Cloning and expression of a novel human brain inward rectifier potassium channel. J Biol Chem 269:20468–20474.

McNicholas CM, Wang W, Ho K, Hebert SC, Giebisch G (1994) Regulation of ROMK1 K^+ channel activity involves phosphorylation processes. Proc Natl Acad Sci USA 91:8077–8081.

Miyake M, Christie MJ, North RA (1989) Single potassium channels opened by opioids in rat locus coeruleus neurons. Proc Natl Acad Sci USA 86:3419–3422.

Morishige K, Takahashi N, Findlay I, Koyama H, Zanelli JS, Peterson C, Jenkins NA, Copeland NG, Mori N, Kurachi Y (1993) Molecular cloning, functional expression and localization of an inward rectifier potassium channel in the mouse brain. FEBS Lett 336:375–380.

Morishige K, Takahashi N, Jahangir A, Yamada M, Koyama H, Zanelli JS, Kurachi Y (1994) Molecular cloning and functional expression of a novel brain-specific inward rectifier potassium channel. FEBS Lett 346:251–256.

Nakajima Y, Nakajima S, Inoue M (1988) Pertussis toxin-insensitive G protein mediates substance P-induced inhibition of potassium channels in brain neurons. Proc Natl Acad Sci USA 85:3643–3647.

North A (1989) Drug receptors and the inhibition of nerve cells. Br J Pharmacol 98:13–28.

Patil N, Cox DR, Bhat D, Faham M, Myers RM, Peterson AS (1995) A potassium channel mutation in weaver mice implicates membrane excitability in granule cell differentiation. Nature Genet 11:126–129.

Paxinos G (1995) The rat nervous system. Sydney: Academic.

Paxinos G, Watson C (1986) The rat brain in stereotaxic coordinates. Sydney: Academic.

Penington NJ, Kelly JS, Fox AP (1993) Unitary properties of potassium channels activated by 5-HT in acutely isolated rat dorsal raphe neurones. J Physiol (Lond) 469:407–426.

Pennefather PS, Heisler S, MacDonald JF (1987) A potassium conductance contributes to the action of somatostatin-14 to suppress ACTH secretion. Brain Res 444:346–350.

Périer F, Radeke CM, Vandenberg CA (1994) Primary structure and characterization of a small-conductance inwardly rectifying potassium channel from human hippocampus. Proc Natl Acad Sci USA 91:6240–6244.

Reuveny E, Slesinger PA, Inglese J, Morales JM, Iniguez-Lluhi JA, Lefkowitz RJ, Bourne HR, Jan YN, Jan LY (1994) Activation of the cloned muscarinic potassium channel by G protein $\beta\gamma$ subunits. Nature 370:143–146.

Sheng M, Tsaur ML, Jan YN, Jan LY (1994) Contrasting subcellular localization of the Kv1.2 K^+ channel subunit in different neurons of rat brain. J Neurosci 14:2408–2417.

Shuck ME, Bock JH, Benjamin CW, Tsai T-D, Lee KS, Slightom JL, Bienkowski MJ (1994) Cloning and characterization of multiple forms of the human kidney ROM-K potassium channel. J Biol Chem 269:24261–24270.

Spauschus A, Lentes KU, Wischmeyer E, Dißmann E, Karschin C, Karschin A (1996) A G protein-activated inwardly rectifying K^+ channel, GIRK4, from human hippocampus associates with other GIRK channels. J Neurosci 16:930–938.

Stanfield PR, Davies NW, Shelton PA, Khan IA, Brammar WJ, Standen NB, Conley EC (1994) The intrinsic gating of inward rectifier K^+ channels expressed from the murine IRK1 gene depends on voltage, K^+ and Mg^{2+}. J Physiol (Lond) 475:1–7.

Stoffel M, Tokuyama Y, Trabb JB, German MS, Tsaar ML, Jan LY, Polonsky KS, Bell GI (1995) Cloning of rat KATP-2 channel and decreased expression in pancreatic islets of male Zucker diabetic fatty rats. Biochem Biophys Res Commun 212:894–899.

Takahashi N, Morishige K-I, Jahangir A, Yamada M, Findlay I, Koyama H, Kurachi Y (1994) Molecular cloning and functional expression of cDNA encoding a second class of inward rectifier potassium channels in the mouse brain. J Biol Chem 269:23274–23279.

Tang W, Yang XC (1994) Cloning a novel human brain inward rectifier potassium channel and its functional expression in *Xenopus* oocytes. FEBS Lett 348:239–243.

VanDongen AMJ, Codina J, Olate J, Mattera R, Joho R, Birnbaumer L, Brown AM (1988) Newly identified brain potassium channels gated by the guanine nucleotide binding protein G_o. Science 242:1433–1437.

Velimirovic BM, Koyano K, Nakajima S, Nakajima Y (1995) Opposing mechanisms of regulation of a G protein-coupled inward rectifier K^+ channel in rat brain neurons. Proc Natl Acad Sci USA 92:1590–1594.

Wang H, Kunkel DD, Martin TM, Schwartzkroin PA, Tempel BL (1993) Heteromultimeric K^+ channels in terminal and juxtaparanodal regions of neurons. Nature 365:75–79.

Wang H, Kunkel DD, Schwartzkroin PA, Tempel BL (1994) Localization of Kv1.1 and Kv1.2, two K channel proteins, to synaptic terminals, somata, and dendrites in the mouse brain. J Neurosci 14:4588–4599.

Wickman KD, Iñiguez-Lluhi JA, Davenport PA, Taussig R, Krapivinsky GB, Linder ME, Gilman AG, Clapham DE (1994) Recombinant G-protein $\beta\gamma$-subunits activate the muscarinic-gated atrial potassium channel. Nature 368:255–257.

Wischmeyer E, Dißmann E, Lentes KU, Karschin A (1995a) 5-HT-induced inhibition via G proteins of an IRK channel cloned from rat basophilic leukemia cells. Soc Neurosci Abstr 21:1325.

Wischmeyer E, Lentes KU, Karschin A (1995b) Physiological and molecular characterization of an IRK-type inward rectifier K^+ channel in a tumour mast cell line. Pflügers Arch 429:809–819.

Yano H, Philipson LH, Kugler JL, Tokuyama Y, Davis EM, Le Beau MM, Nelson DJ, Bell GI, Takeda J (1994) Alternative splicing of human inwardly rectifying K^+ channel ROMK1 mRNA. Mol Pharmacol 45:854–860.

Yatani A, Codina J, Sekura RD, Birnbaumer L, Brown A (1987) Reconstitution of somatostatin and muscarinic receptor mediated stimulation of K^+ channels by isolated G_K protein in clonal rat anterior pituitary cell membranes. Mol Endocrinol 1:283–289.

Zhou H, Tate SS, Palmer LG (1994) Primary structure and functional properties of an epithelial K channel. Am J Physiol 266:C809–C824.